ACS Sustainable Chemistry & Engineering

pubs.acs.org/journal/ascecg

Research Article

Cellulose Luminescent Hydrogels Loaded with Stable Carbon Dots for Duplicable Information Encryption and Anti-counterfeiting

Juan Wang, Peng Du, Yu-I Hsu,* and Hiroshi Uyama*

Cite This: https://doi.org/10.1021/acssuschemeng.3c01838

Read Online

ACCESS | Metrics & More | Article Recommendations | Supporting Information

ABSTRACT: Luminescent hydrogels with flexibility and biocompatibility have attracted considerable interest in anti-counterfeiting application. However, conventional luminous substance is prone to release into the surrounding environment, causing accumulation and biotoxicity. The green synthesis of repeatable fluorescent materials from biomass remains challenging. Herein, we report the assembly of nano-cellulose hydrogel doped with naturally originated and multiple active sited carbon dots (CDs) and demonstrate the sustainable usage of information encryption. The problem of CDs leaching from the hydrogel matrix was solved *via* strong chemical interactions between the CDs and cellulose nanofibers. The facilely prepared hydrogels showed extraordinary mechanical properties and fatigue resistance (i.e., the stress, compressive modulus, and compressive toughness were up to 1607.30 kPa, 368.33 kPa, and 191.54 kJ/m^3, respectively). Furthermore, this cellulose-based gel displayed bright green fluorescence under UV light, which could be quenched by Fe^{3+} ions and recovered in an ascorbic acid/EDTA-2Na mixture solution. Therefore, coded information can be easily input and interpreted *via* ionoprinting technique, realizing a simple display and erasing procedure. This elaborately designed biomimetic hydrogel can serve as effective communication media to improve security and expand critical applications in optoelectronic storage devices.

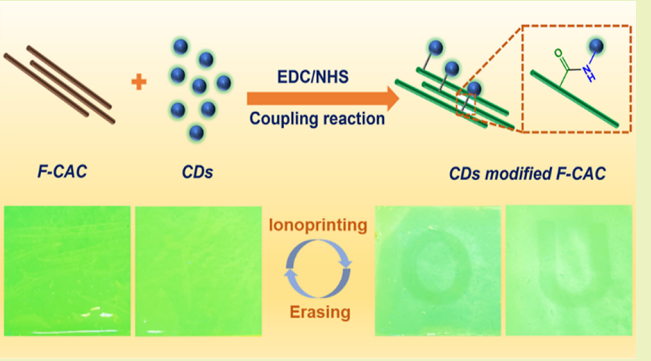

KEYWORDS: *carbon dots, cellulose modification, fluorescent hydrogels, ionoprinting, repeatable encryption*

INTRODUCTION

The rapid development of information techniques greatly improves the convenience of human life but leads to endless counterfeit products and information leakage.[1−3] This trend is contrary to the principles of sustainable development and has resulted in huge waste of the earth's resources. It is an inevitable topic that development of information storage materials with protection and encryption ability.[4] Although considerable research on information encryption materials, including fluorescent ink,[5,6] self-erasing materials,[7,8] and luminescent patterns[9] has been conducted in recent years, flexible smart gels based on discoloration behavior have been scarce. Sustainable and cost-effective hydrogels exhibit unique fluorescent properties and biocompatibility, which are generally exploited in the fields of pharmaceutical industries, imaging, biosensing, therapeutics, and so on.[3,10−12]

It is clear that smart hydrogels are promising candidates for information storage due to their unique responsiveness to specific stimuli, which can load and decrypt hidden information under specific conditions.[13,14] Chen et al.[15] designed a multi-responsive nanofiber-reinforced poly(*N*-isopropyl acrylamide) hydrogel inspired by a paper structure. This hydrogel exhibited solvent-induced high-resolution reversible information recording, self-encryption, and multiple-decryption functions. Lou et al.[16] prepared a polymer hydrogel based on lower critical solution temperature and upper critical solution temperature, which can perform "double locking" from the time and temperature dimensions and can be used for information camouflage and multilevel encryption. Liu et al.[17] innovatively combined the transparency of ion-conducting hydrogels with anti-swelling and macroscopic changes induced by hydrophobic polymer chains in organic hydrogels and prepared ionic organic hydrogels with excellent mechanical properties and unique behaviors (information recognition and encryption) in various environments. These hydrogels can be used as dynamic information storage devices for recording and encrypting information. Owing to attracting great attention, they have been proven to be eminent candidates for flexible anti-counterfeiting in high-level information security.

Received: March 28, 2023
Revised: June 8, 2023

However, the expensive price, lack of eco-friendliness, and incompatibility with hydrogel matrix of fluorescent monomers limit the further development of fluorescent smart hydrogels in this field.[18,19] Recently, carbon dots (CDs) has been widely known as a promising luminescent nanomaterial with abundant low-cost sources, facile synthetic methods, excellent biocompatibility, high chemical stability, significant water solubility, low cytotoxicity, and excellent optoelectronic properties, attracting great attention in many fields including biomedicine, catalysis, optoelectronic devices, and especially anticounterfeiting.[20−22] Many scholars demonstrated that integrating CDs into desirable polymer matrix is a cost-effective and environmentally friendly method to develop flexible materials for information encryption. For instance, Xiong et al. reported a flexible right-hand chiral fluorescent film with potential applications in sensing and anti-counterfeiting.[23] The self-assembled film by CDs-modified cellulose nanocrystals could generate specific fluorescent patterns by two-dimensional chemical printing technology. Wu et al. fabricated double-layer fluorescent hydrogel-organogel with adjustable amphiphilic imidazolium-type ionic liquid-based CDs, and the gel exhibited a light and force dual-stimuli response and could provide more secure information encryption than traditional single-layer encryption materials.[24] Nevertheless, few reports concerned the heterogeneous distribution and even leaching behavior of CDs inside the polymer network due to their weak supramolecular interactions.[25]

The hydrophilic polymer chain in hydrogel is beneficial for the homogeneous dispersion of high-water soluble CDs. Further, the abundant functional groups, such as carboxyl, amino, hydroxyl, etc. on CDs surface provide the possibility of chemical fixation inside the hydrogel matrix. On the one hand, three-dimensional (3D) networks of hydrogel can provide the CDs with chemical stability, also contribute to inhibit the aggregation-caused-quenching (ACQ) effect of high concentration CDs.[26] On the other hand, the introduced CDs improves the mechanical properties of the hydrogel as well as confers the material additional functionality such as information storage and anti-counterfeiting.[27]

Based on the concepts of a green economy and sustainable development, the utilization of natural renewable resources as CDs carriers is a reasonable choice.[11,28] Cellulose, a plant-based renewable fiber, has been chosen as an environmentally friendly hydrogel material because of its distinguishable mechanical properties, multi-hydroxy functionality, biodegradability, and abundant availability.[29,30] The presence of massive functional groups and charges in cellulose backbone provides the opportunity of modification reactions. Lv et al.[31] used the physical electrostatic interaction between carboxymethyl cellulose and CDs to uniformly disperse CDs into a hydrogel matrix to obtain fluorescent hydrogels with excellent mechanical properties that can be used to store information and anti-counterfeiting. Hence, it not only provides a backbone for the assembly of 3D structure, but also serves as a natural holder to introduce CDs uniformly into the hydrogel matrix.

In this research, we report a facile fabrication of chemistry bonding fluorescent nanocomposite hydrogel based on green-synthesized CDs and fibrillated citric acid-modified cellulose (F-CAC). Through the stupendous chemical interaction between the CDs and F-CAC, CDs/F-CAC was incorporated into a biocompatible, flexible hydrogel matrix of acrylamide and the hydroxyethyl methyl acrylate copolymer, P(AAm-*co*-HEMA). Thus, the CDs/F-CAC chains enabled the composite gel to overcome the shortcomings of nanoparticle leaching, avoiding the migration of CDs outside the gel when swollen. The CDs/F-CAC not only significantly improved the mechanical properties and anti-fatigue performance of P(AAm-*co*-HEMA) but also endowed the hydrogels with excellent fluorescence properties. Satisfyingly, the fluorescence of the CDs/F-CAC hydrogels was quenched by Fe^{3+} ions and recovered in an ascorbic acid/EDTA-2Na mixture solution. Thus, the as-prepared display platform of fluorescent hydrogel *via* ionoprinting technique could be used repeatedly. This novel strategy broadens the applications of natural resources hydrogels as storage modules for information encryption and anti-counterfeiting.

EXPERIMENTAL SECTION

Materials. Citric acid, urea, acrylamide (AAm), ascorbic acid, ammonium persulfate (APS), and iron chloride hexahydrate ($FeCl_3 \cdot 6H_2O$) were purchased from Wako Pure Chemical Industries, Ltd. (Wako, Osaka, Japan). Cellulose [microcrystalline powder, particle size of 51 μm, and bulk density of 0.6 g/mL (25 °C)] was purchased from Sigma Co., Ltd. (Aldrich, USA). 1-(3-Dimethylaminopropyl)-3-ethylcarbodiimide hydrochloride (EDC) and *N*-hydroxysuccinimide (NHS), were obtained from Tokyo Chemical Industry Co., Ltd. (TCI, Tokyo, Japan). Methanol, acetone, 0.1 mol/L acetate buffer solution (pH = 5), 2-hydroxyethyl methacrylate (HEMA), and *N*, *N*′-methylenebisacrylamide (MBAA) were purchased from Nacalai Tesque, Inc. (Kyoto, Japan). EDTA-2Na was purchased from Dojindo Laboratories Co., Ltd. (Kumamoto, Japan). All chemicals were used without further purification. Deionized (DI) water purified using a Milli-Q system (Millipore Inc., Milford, MA) was used in all experiments.

Synthesis of Fluorescent CDs. Luminescent CDs were synthesized *via* one-step microwave pyrolysis.[32] Briefly, citric acid (3 g) and urea (3 g) were dissolved in DI water (10 mL), and the clarified solution was obtained under ultrasonic vibration. Next, the transparent solution was placed in a domestic microwave oven (Panasonic, Japan) and heated using middle−high fire (600 W) for approximately 7 min. The obtained brown-black solid was dissolved in an appropriate amount of water and centrifuged (10,000 rpm, 20 min) to remove large insoluble solid particles. Furthermore, the CDs solution was dialyzed using a dialysis membrane (MWCO = 1000) in DI water for 48 h to remove unreacted starting materials and small-molecular-weight reaction products. Finally, the CDs were obtained as a dark brown solid after rotary evaporation and dried under vacuum.

Modification and Fibrillation of Cellulose. Citric acid-modified cellulose (CAC) was prepared using a method similar to that reported in our previous work.[33] Briefly, microcrystalline cellulose powder (30 g) was dispersed in DI water (300 mL), and citric acid (90 g) was added to the cellulose solution under strong stirring. After the citric acid was completely dissolved, the mixture was transferred into an oven at 130 °C for 15 h, and the esterification reaction occurred with the evaporation of water under high temperatures. After the reaction, the modified cellulose was processed with filtration and washed with DI water to remove residual citric acid until the filtrate was neutral. The product was washed with methanol and acetone. CAC was obtained after 1 day of vacuum drying. To obtain a fibrillated and homogeneous suspension of CAC nanofibers, an aqueous suspension of CAC (1.5 wt %) was prepared and then pulverized using a Star Burst Mini wet pulverizing and dispersing device (Sugino Machine Co., Ltd., Japan). Under an ejection pressure of 245 MPa, the CAC mechanically disintegrated into cellulose nanofibers 30 times, and the prepared aqueous suspension was named F-CAC (1.5 wt %).

The carboxylic-group content of the F-CAC was measured by conductometric titration using a conductivity meter (LAQUA F-74; HORIBA Ltd., Kyoto, Japan). The average carboxyl content was 0.48 mmol/g, calculated according to a previously reported test method.[34]

https://doi.org/10.1021/acssuschemeng.3c01838
ACS Sustainable Chem. Eng. XXXX, XXX, XXX−XXX

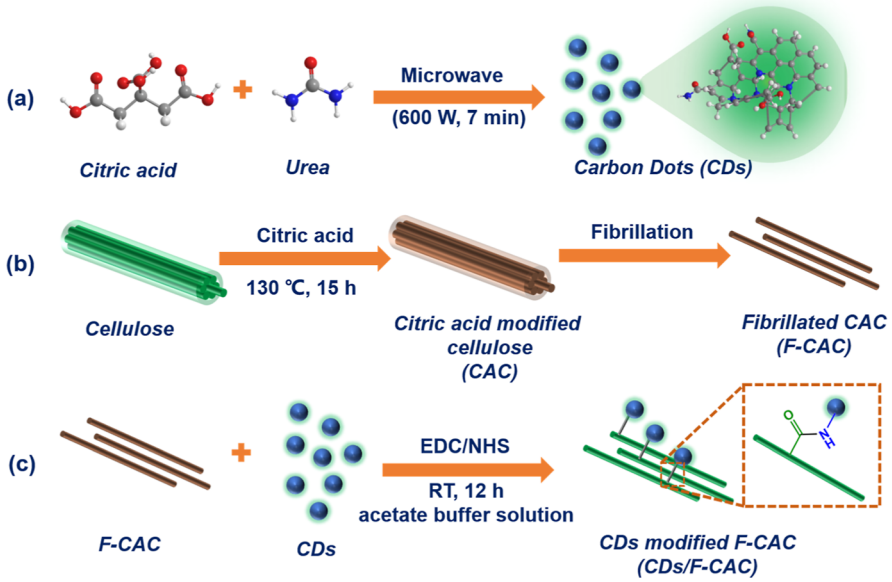

Figure 1. Schematic illustration of the preparation of (a) CDs, (b) F-CAC, and (c) CDs/F-CAC.

Preparation of CAC Nanocomposite Decorated with CDs (CDs/F-CAC). The F-CAC was further decorated with CDs based on common EDC/NHS coupling chemistry, according to previous reports.[28] First, the F-CAC aqueous solution (40 mL, 1.5 wt %) was added to 20 mL acetate buffer solution (0.1 M, pH = 5) with ultrasonic vibration for 30 min. Next, EDC (119 mg) was added, and the admixture was vigorously stirred for 15 min. Subsequently, NHS (460 mg) was added, and the admixture was continuously stirred for 15 min. Then, 100 mg of the CDs was added to the reaction mixture. The reaction proceeded overnight under magnetic stirring at room temperature (RT) in the dark. The resulting suspension was dialyzed (MWCO = 1000) in DI water for 48 h. After freeze-drying, a light-brown powder was obtained and named CDs/F-CAC.

Preparation of Fluorescent Hydrogels. Fluorescent hydrogels were prepared *via* one-pot free-radical polymerization of the precursor aqueous solution within HEMA, AAm, CDs/F-CAC, and MBAA, using APS as the initiator. The procedure was as follows: initially, we dissolved a certain amount of CDs/F-CAC in 5 mL DI water and sonicated it until uniformly dispersed. Subsequently, 2 g HEMA, 1 g AAm, 30 mg APS, and 15 mg MBAA were added to the solution, sonicated, and stirred until a homogeneous solution was obtained. After degassing by bubbling with nitrogen for 10 min, the mixture was injected into a self-made mold consisting of two glass plates and one silica plate (2 mm). In situ free-radical polymerization of the hydrogel was performed in a water bath at 60 °C for 6 h. The hydrogels were named CDs/F-CAC-0.1, CDs/F-CAC-0.5, CDs/F-CAC-1.0, and CDs/F-CAC-1.5 with the CDs/F-CAC content varying from 0.1 wt % to 0.5, 1.0, and 1.5 wt %, respectively (based on the total weight of HEMA and AAm). At the same time, the same method was used to prepare hydrogel without CDs/F-CAC and named CDs/F-CAC-0. The hydrogels containing only CDs, which have the same quality as the CDs with the CDs/F-CAC-1.0 hydrogel according to the loading content of CDs, were synthesized *via* the same procedure and named CDs-1.0.

Information Loading and Erasing. Information was loaded into hydrogels using ionoprinting, as reported by Le et al.[35] Briefly, the filter papers were soaked in $FeCl_3$ solution (125 mM) for 2 h, then removed and dried in an oven (60 °C). After drying, the filter papers containing Fe^{3+} were cut into the desired shapes and then placed on the surface of the fluorescent hydrogels for 2 min. After peeling off the filter paper, the desired information loading was obtained and visualized under specific UV light. The information-loaded hydrogels were soaked in a mixed solution of ascorbic acid/EDTA-2Na (0.1 M) for 2 h, and the information was erased.

Characterization. Attenuated total reflection Fourier-transform infrared (ATR-FTIR) spectroscopy (Thermo Scientific Nicolet iS5, USA), UV−vis absorption spectroscopy (J-820 AC, JASCO Corporation, Japan), X-ray diffraction (XRD, Rigaku Corporation, Tokyo, Japan), and X-ray photoelectron spectroscopy (XPS, JEOL JPS-9010MC) were used to confirm the chemical compositions and structures of the CDs, CAC, and CDs/F-CAC. The light transmittance measurement of the hydrogels was conducted in quartz cells through UV−vis spectrophotometer. The heights and morphologies of the CDs and F-CAC were characterized using atomic force microscope (AFM, SPI3800N/SPA-400, Seiko Instruments Inc., Tokyo, Japan). The microstructures and morphologies of the cellulose, F-CAC, and hydrogels were observed using scanning electron microscopy (SEM, Hitachi SU-3500, Japan). The photoluminescence (PL) spectra of the CDs and hydrogels were recorded using a microplate reader (SH-9000Lab, Yamato Scientific Co., Ltd., Tokyo, Japan). The thermal stability of the CDs, CAC, and CDs/F-CAC was investigated using a thermogravimetric analyzer (TGA, Hitachi STA7200RV, Japan) by heating from 30 to 800 °C under nitrogen protection.

Swelling Measurements. The swelling behavior of the as-prepared gels was measured in a large amount of DI water at RT until swelling equilibrium was reached. At certain times, the gels were removed surface water and quickly weighed. The swelling ratio (SR) was calculated as, $SR = (W_s - W_d) \times 100\%/W_d$, where W_s and W_d are the weights of the swollen hydrogels and the corresponding dried hydrogels, respectively.

Mechanical Tests. The samples for the compression and cyclic compression tests were prepared in cylindrical shapes with length of 8−10 mm and a diameter of 13 mm. The stress at the respective compression strains on the hydrogels was characterized using an EZ Graph universal material testing machine (Shimadzu, Japan) equipped with a 500 N load and a speed of 3.0 mm/min at RT. The compressive modulus was determined from the slope of the nominal compression curve in the strain range of 10−20%. The compressive toughness U_{CT} was estimated from the area under the stress−strain curve, using the following equation

$$U_{CT} = \frac{\int_0^{0.7} F\,ds}{\pi R^2} \quad (1)$$

where F is the compressive load and s is the compressive displacement of the corresponding strain. For the self-recovery experiment, successive loading−unloading compression tests were performed 10

https://doi.org/10.1021/acssuschemeng.3c01838
ACS Sustainable Chem. Eng. XXXX, XXX, XXX−XXX

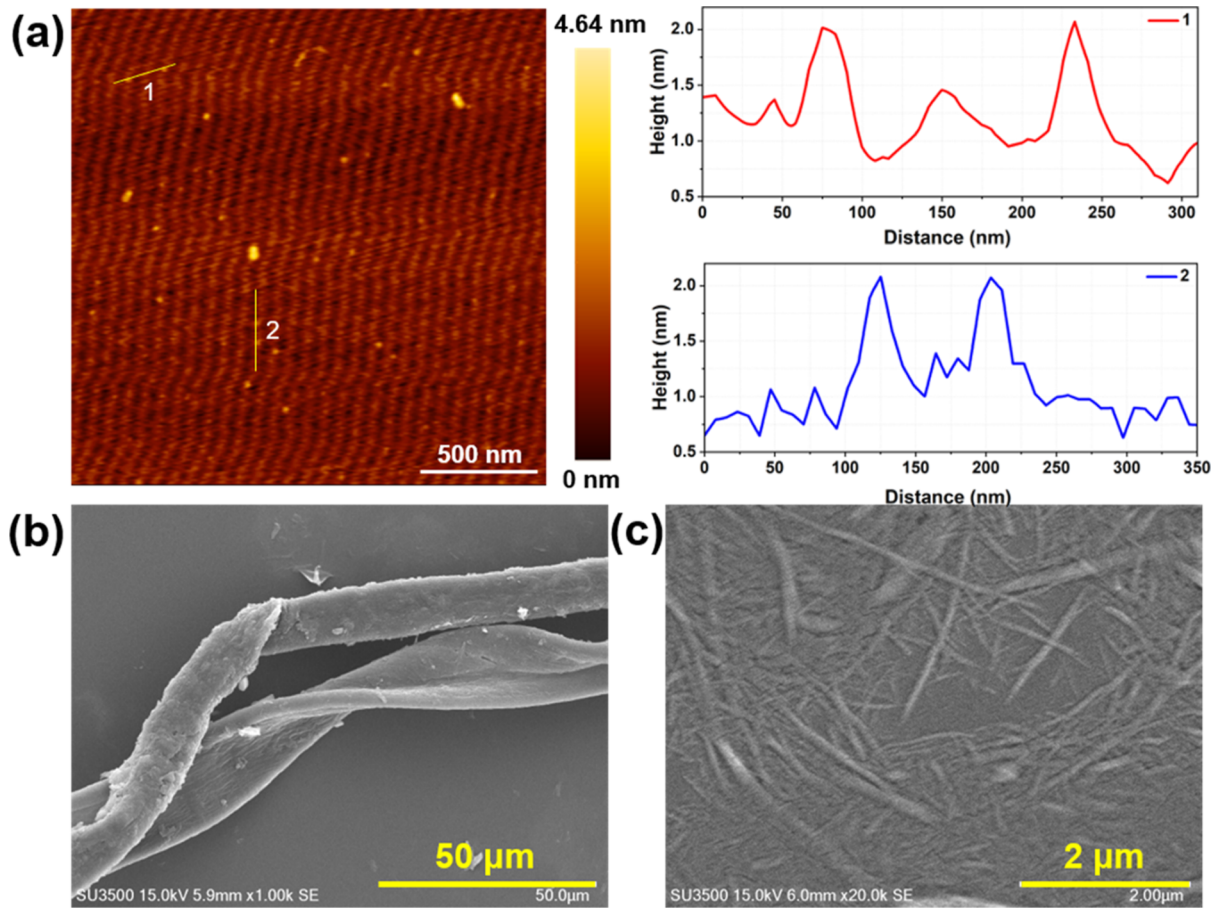

Figure 2. (a) AFM (on mica) image and topography of CDs. SEM image of (b) cellulose and (c) F-CAC.

times under different strains (10, 30, and 50%) at a rate of 0.5 mm/min and tested again with a resting time (1 min). The hysteresis energies were calculated from the loop area between the loading and unloading curves.

Rheological Properties. Rheological tests were performed using a Haake Rheostress 6000 (Thermo Fisher Scientific, Waltham, MA, USA) instrument equipped with 20 mm-diameter parallel plates to analyze the gels at RT. The angular frequency was swept from 1 to 100 rad/s at a fixed strain of 0.1%.

RESULTS AND DISCUSSION

Synthesis of Materials. The CDs were prepared by heating citric acid and urea in DI water *via* a one-step microwave method, as shown in Figure 1a. Microwave irradiation technology is an efficient option because of its advantages of in situ, instantaneous heating, and large-scale synthesis of homogeneous CDs.[36] We demonstrated that the resulting CDs could be homogeneously dispersed in DI water, producing a dark brown solution, as shown in Figure S1. The CDs exhibited significant dispersibility when a one-step microwave method was used.

To enhance the functionality and hydrophilicity, citric-acid-modified cellulose was prepared to endow the surface with carboxylic acid groups, which can serve as reactive sites, as shown in Figure 1b. The modification was achieved through esterification between the hydroxyl groups of cellulose and carboxyl groups of citric acid. Because the modification reaction was carried out in the solid state, it allowed the mass production of modified cellulose without using organic solvents. To prepare nanocellulose, a fibrillation method that uses aqueous counter collision (ACC) without any chemical modification was used to increase the surface area of CAC for the next reaction.[37] Figure 1c displays amino-carrying CDs grafted onto F-CAC using common EDC/NHS coupling chemistry.

Micro-morphology of CDs. In general, AFM was used to confirm the morphologies and heights of the prepared CDs, as shown in Figure 2a. The CDs were uniformly sized spheres with a height of approximately 2−3 nm. The surface morphologies of the cellulose and fibrillated cellulose were compared using SEM. It can be seen from Figure 2b that the cellulose is coarse and intertwined. Comparatively, after treatment with ACC for 30 passes, cellulose was crushed into nanoscale fragments, as shown in Figure 2c, which is consistent with the AFM results for F-CAC (Figure S2).

Characterization of Materials. FTIR spectroscopy was used to detect the occurrence of the reaction (Figure 3a). Compared to the characteristic spectra of cellulose, esterification by citric acid was determined by the presence of new carboxylic acid and ester carbonyl peaks at approximately 1730 cm^{-1}. The CDs exhibited stretching vibrations of C−OH at 3204 cm^{-1}, C−H at 3057 cm^{-1}, and C−N or C−O−C at 1281 cm^{-1}. The peaks centered at 1584 and 1694 cm^{-1} are attributed to the N−H and C=O bonds, respectively. The existence of these broad absorption bands demonstrates the presence of functional groups, such as carboxyl and amide, on the surface of CDs.[31] Compared to the spectrum of F-CAC, the characteristic bands at 1580 (corresponding to the $-NH_2$ stretching vibration of excess CDs) and 1704 cm^{-1}

https://doi.org/10.1021/acssuschemeng.3c01838
ACS Sustainable Chem. Eng. XXXX, XXX, XXX−XXX

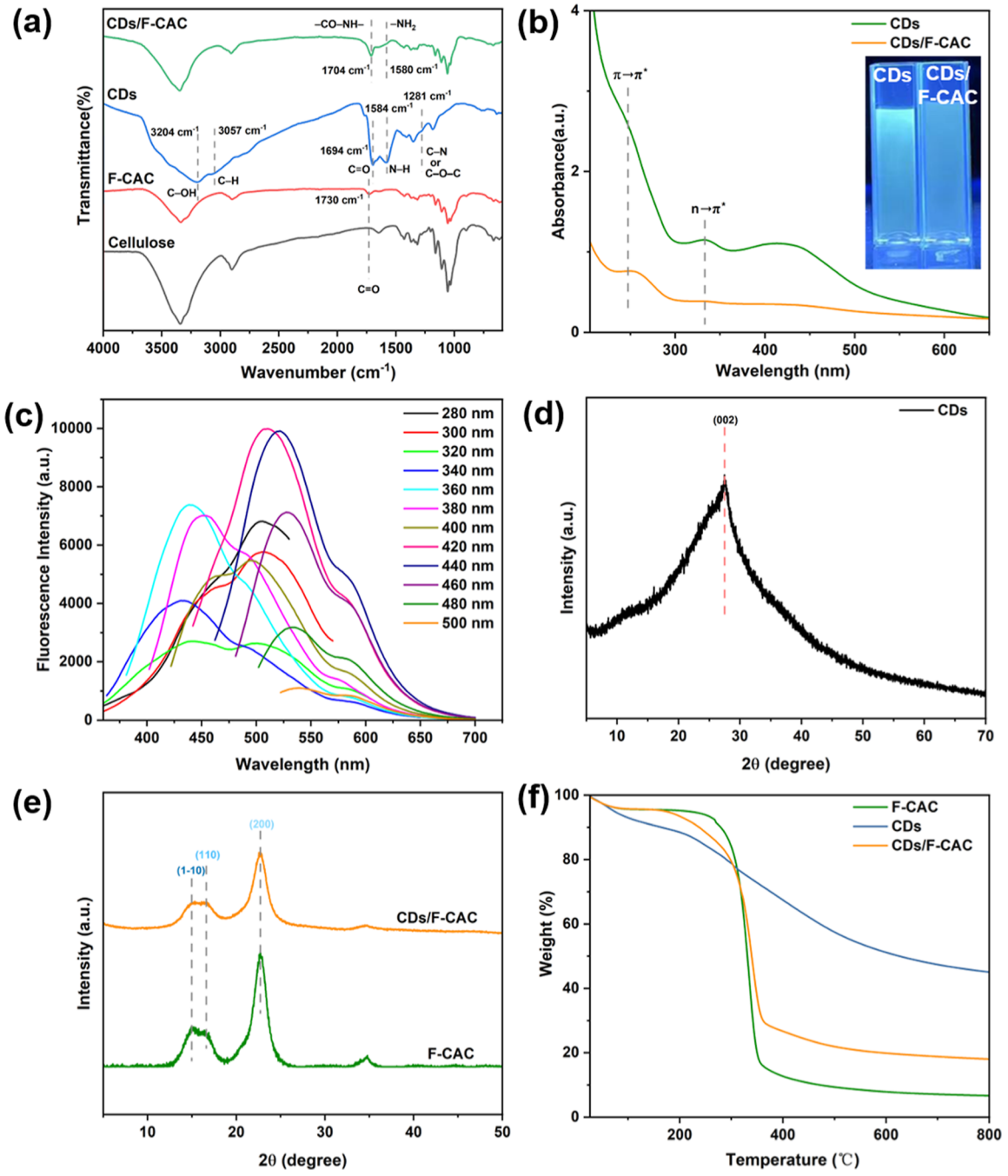

Figure 3. (a) ATR-FTIR spectra of cellulose, F-CAC, CDs, and CDs/F-CAC. (b) UV−vis absorption spectra of CDs and CDs/F-CAC. Insets show photographs of CDs and CDs/F-CAC solutions under 365 nm UV lamp. (c) PL spectra of the CDs under different excitation wavelengths. XRD patterns of (d) N-CDs, (e) F-CAC, and CDs/F-CAC. (f) TGA thermogram of F-CAC, CDs, and CDs/F-CAC.

(corresponding to the −CO−NH− stretching vibration) were observed in the spectrum of CDs/F-CAC. This verifies the occurrence of carboxyamine condensation between F-CAC and CDs.

The aqueous solutions of CDs and CDs/F-CAC emit green light with excitation occurring at λ_{ex} = 365 nm (under UV lamp), indicating obvious fluorescence, as shown in the inset of Figure 3b. In Figure 3b, the UV−vis spectra of CDs and CDs/F-CAC show nearly the same characteristic absorption peaks, including distinct absorption shoulders at ≲250 nm, clear peaks at 340 nm, and shoulders located at 440 nm. Based on the literature, absorption bands at approximately 250 nm are attributed to a $\pi-\pi^*$ transition of the C=C and C=N bonds of the sp^2 C domain in polymetric carbon nitrides, and the peaks at 340 nm are assigned to the $n-\pi^*$ transition of the C=O and C=N bonds in g-C_3N_4, corresponding to a typical absorption pattern of carbon nitride (335 nm).[38] The extended absorption shoulders located at 440 nm may result from the complex ligand shell at the CDs surface and which is known as surface state transition.[39,40]

In the fluorescence spectra, the CDs exhibited an emission intensity maximum at 510 nm when excited at 420 nm (Figure S3). Similar to previous reports,[36,41,42] the CDs showed an obvious dependence of the PL wavelength and intensity on the

https://doi.org/10.1021/acssuschemeng.3c01838
ACS Sustainable Chem. Eng. XXXX, XXX, XXX−XXX

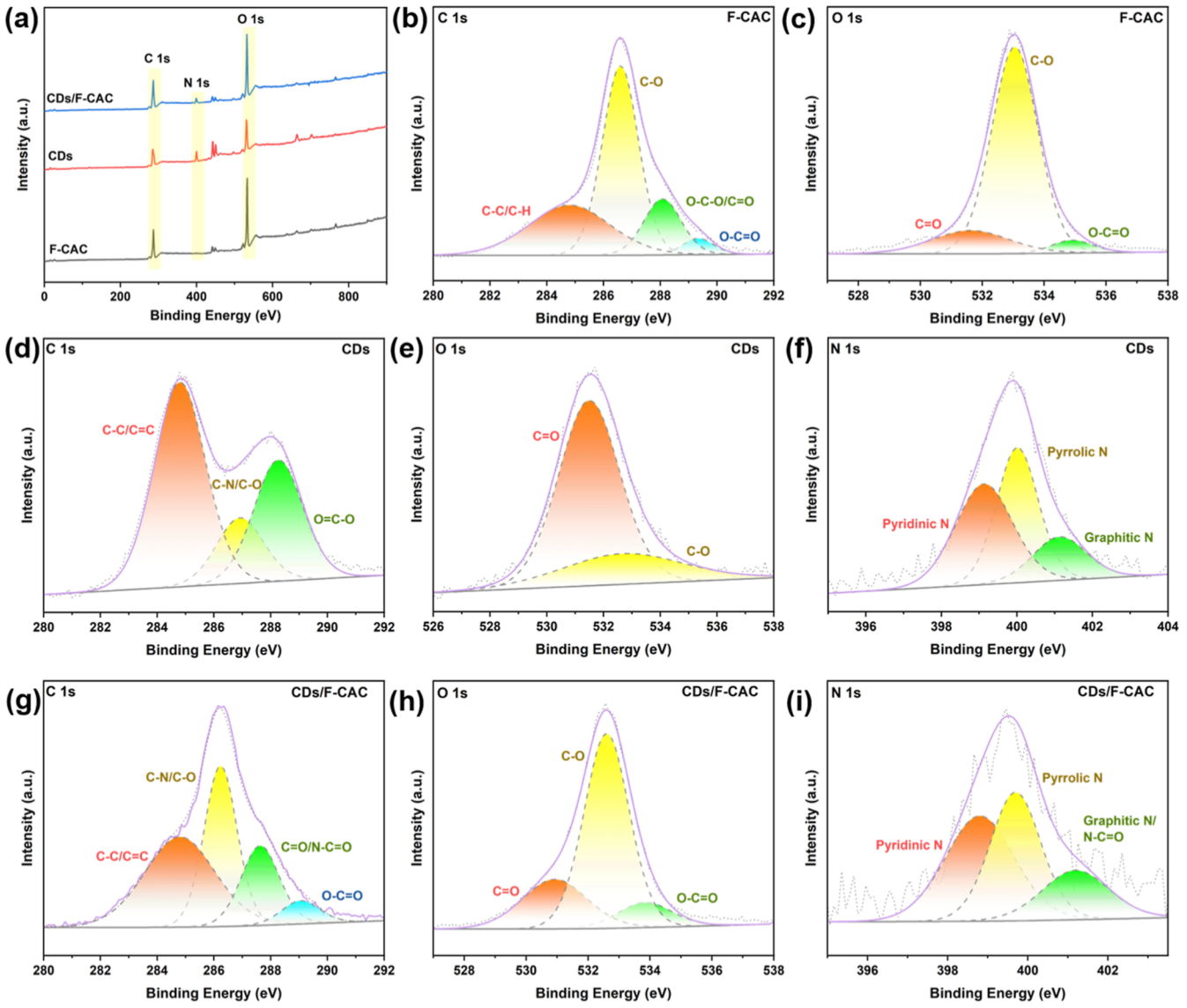

Figure 4. (a) XPS survey spectra of F-CAC, CDs, and CDs/F-CAC. (b–c) High-resolution XPS fitting results for C 1s and O 1s of F-CAC. (d–f) High-resolution XPS fitting results for the C 1s, O 1s, and N 1s spectra of CDs. (g–i) High-resolution XPS fitting results for the C 1s, O 1s, and N 1s spectra of CDs/F-CAC.

excitation wavelength (Figure 3c), which is a typical characteristic of fluorescent carbon materials and may be due to the presence of core carbon, diverse surface states (hybridization between the core carbon and functional groups), and molecular states owing to the presence of phosphors. Moreover, the photobleaching tolerance inherited from F-CAC assisted CDs/F-CAC in retaining over 97.43% of original luminescence intensity under 120 min UV irradiation as shown in Figure S4, which proved the strong anchoring ability of F-CAC.

The wide (002) peak at around 27° of the XRD diffraction pattern of the CDs demonstrates that carbonized citric acid and urea can produce the graphite structure, as shown in Figure 3d.[43] In Figure 3e, the XRD diffraction patterns of F-CAC and CDs/F-CAC demonstrate the unique diffraction regions of **cellulose I**. The main peaks at 14.9, 16.4, and 22.5 were attributed to the typical (110), (110), and (200) reflections of the **cellulose I** pattern, respectively.[44] Compared to that of F-CAC, the XRD pattern of CDs/F-CAC did not change significantly, implying that the typical structure of **cellulose I** was maintained even though CDs were attached to the surface of F-CAC *via* an acylation reaction.[45]

Thermogravimetric analysis was utilized to verify the thermal stability of CDs, F-CAC, and CDs/F-CAC and to determine the loading content of the CDs. Figure 3f shows TGA curves of the test samples. The weight loss rate during the test can be calculated using the following formula

$$W = \frac{W_{\text{initial}} - W_{\text{end}}}{W_{\text{initial}}} \times 100\% \quad (2)$$

where W_{initial} is the initial quality of the test and W_{end} is the final amount.

The initial small weight loss was caused by the evaporation of low-molecular-weight compounds or adsorbed water from the curves. At first, the CDs began to decompose with increasing temperature, which could be attributed to the decomposition caused by unsteady oxygenous groups on the loose surface of the CDs and CO, CO_2, and other oxygenated carbides that were simultaneously generated. This is why CDs/

https://doi.org/10.1021/acssuschemeng.3c01838
ACS Sustainable Chem. Eng. XXXX, XXX, XXX−XXX

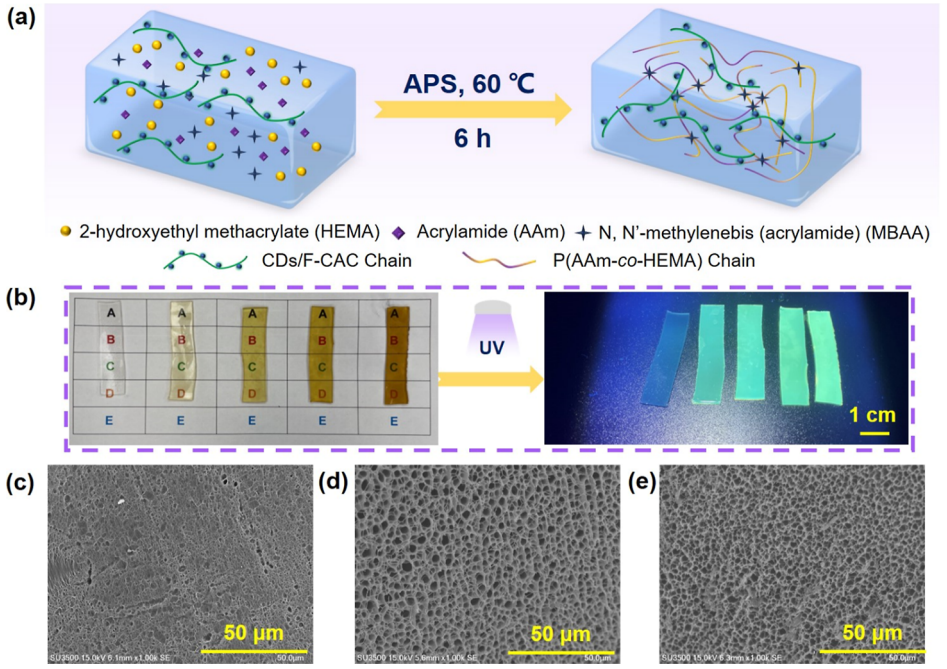

Figure 5. (a) Schematic illustration of the synthetic process of CDs/F-CAC hydrogels. (b) Appearance of CDs/F-CAC hydrogels with different concentrations under visible and UV light (from left to right: CDs/F-CAC-0, CDs/F-CAC-0.1, CDs/F-CAC-0.5, CDs/F-CAC-1.0, and CDs/F-CAC-1.5). Cross-sectional SEM images of the freeze-dried CDs/F-CAC hydrogels: (c) CDs/F-CAC-0, (d) CDs/F-CAC-0.1, and (e) CDs/F-CAC-0.5.

F-CAC decomposes earlier than F-CAC. It is clear that at 800 °C, the mass loss of the CDs/F-CAC composite was lower than that of F-CAC. This may be because the stable CDs did not participate in combustion; only the macromolecules were involved in combustion, indicating the successful loading of CDs on the F-CAC. Moreover, the loading of CDs had little effect on the thermal degradation behavior of cellulose, which further confirms the successful synthesis of CDs/F-CAC nanocomposites.[46] Based on the weight loss rate calculations, the loading content of CDs was approximately 34%.

XPS was used to analyze the surface chemical compositions, structures, and bonds of the prepared hybrid materials. The full XPS profiles of F-CAC, CDs, and CDs/F-CAC, as well as their corresponding elemental contents, are shown in Figure 4a and Table S1. The C 1s, O 1s, and N 1s fine spectra of the samples were analyzed in detail (Figure 4b−i). The compositions of the elements and their corresponding contents are shown in Figure 4a and listed in Table S1. The XPS spectra show that F-CAC is composed of C and O elements with binding energies of 286.2 and 533.2 eV attributed to C 1s and O 1s, respectively. For the CDs and CDs/F-CAC, in addition to C and O, the full-scan XPS spectra presents distinct N 1s peaks at 399.3 eV. Table S1 shows that the CDs present a higher N and C atomic ratios (11.759 and 59.795%, respectively) and lower O/C ratio (0.48) than those of F-CAC, indicating that a high fraction of N atoms were successfully doped into the CDs.[47] The N atomic ratio decreases to 6.76% after conjugating the CDs with F-CAC (to form CDs/F-CAC hybrids). Moreover, comparing F-CAC with CDs/F-CAC, the O/C ratio decreases from 0.73 to 0.66, which can be taken as a further indication of a successful coupling reaction. Furthermore, a detailed analysis of the C 1s, O 1s, and N 1s peaks of F-CAC, CDs, and CDs/F-CAC was performed. As expected, combined with the detailed XPS spectra of F-CAC and CDs (Figure 4b−f), the C 1s, N 1s, and O 1s spectra of CDs/F-CAC verify the occurrence of an acylation reaction.[45] The C 1s spectra (Figure 4g) suggest the presence of C−C/C=C (284.8 eV), C−N/C−O (286.2 eV), C=O/N−C=O (287.6 eV), and O−C=O (289.1 eV). The O 1s spectra (Figure 4h) are deconvoluted into three peaks at 530.9, 532.6, and 533.8 eV corresponding to C=O, C−O, and O−C=O, respectively. The N 1s spectra (Figure 4i) can be divided into three peaks at 398.8, 399.7, and 401.2 eV, which can be assigned to pyridinic N, pyrrolic N, and graphitic N/N−C=O, respectively. Therefore, it can be concluded that CDs/F-CAC is mainly composed of carbon atoms and oxygen- and nitrogen-containing functional groups.[48,49]

Synthesis and Morphologies of CDs/F-CAC Hydrogels. The preparation of the hydrogels with fluorescent properties is illustrated in Figure 5a. F-CAC provided the natural skeleton that connected with the fluorescent CDs based on a carboxyamine condensation reaction, and hydrogels were then prepared through the one-pot free radical copolymerization method. Rigid F-CAC enhances the mechanical properties of the hydrogels, whereas CDs impart fluorescence properties to them. The as-prepared hydrogels with a thickness of 1 mm (Figure 5b) displayed increasing green fluorescence under UV light as the CDs/F-CAC content increased. By contrast, the transparency of the hydrogels gradually decreased from 93 to 80% with an addition of less than 1.0 wt % (Figure S5). However, the 1.5 wt % of CDs/F-CAC were difficult to homogeneously disperse in hydrogel matrix, resulting in a light transmittance below 50%. The cross-sectional morphologies of the freeze-dried hydrogels with different CDs/F-CAC contents are shown in Figure 5c−e. Compared to the hydrogel without the addition of CDs/F-CAC (Figure 5c), the CDs/F-CAC-0.1 (Figure 5d) and CDs/F-CAC-0.5 (Figure 5e) hydrogel cross-sections have more regular pore channels and homogeneous structures with tighter networks, which may lead to outstanding mechanical properties of the CDs/F-CAC hydrogels. Interestingly, numerous

https://doi.org/10.1021/acssuschemeng.3c01838
ACS Sustainable Chem. Eng. XXXX, XXX, XXX−XXX

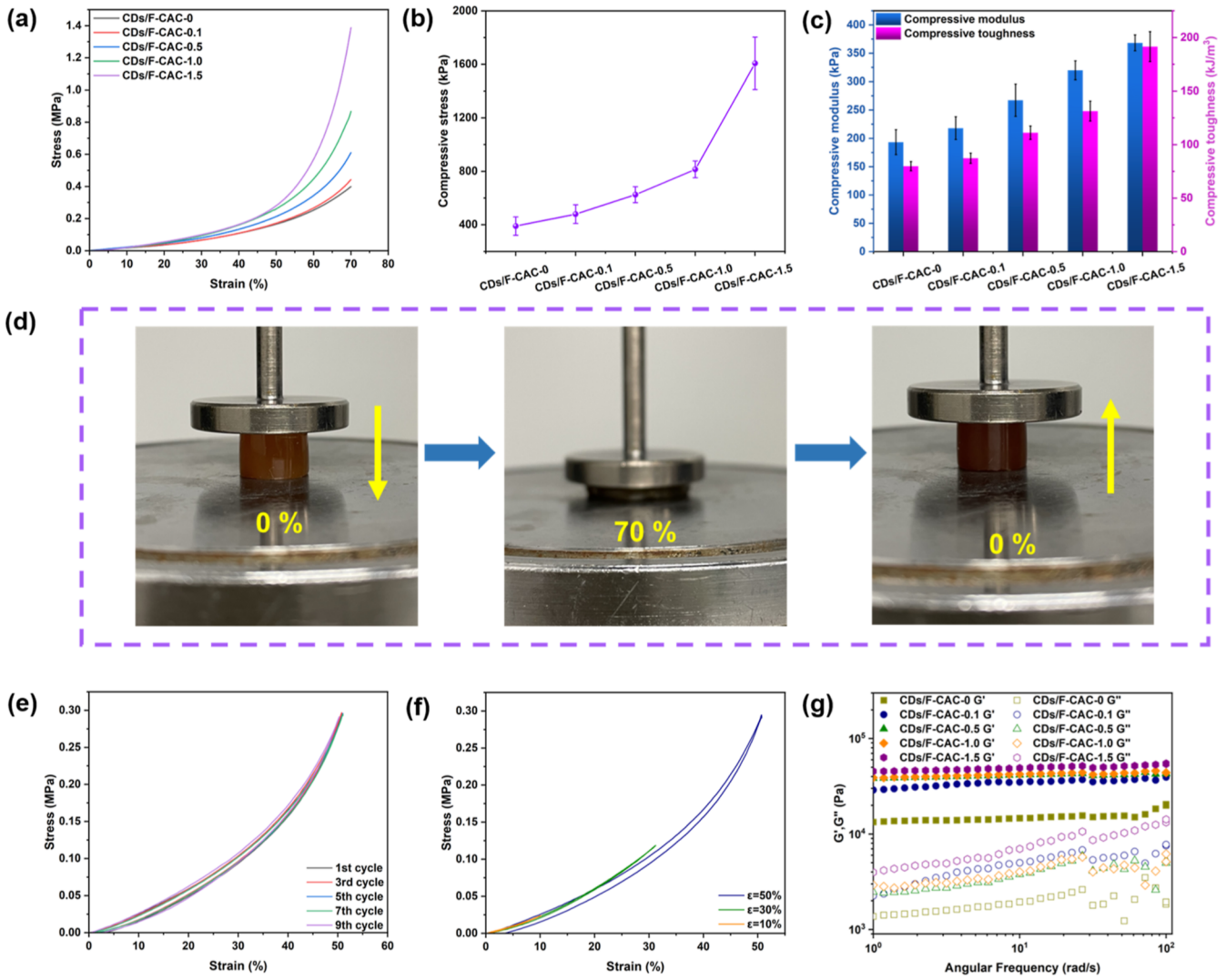

Figure 6. (a) Compressive curves of hydrogels with different CDs/F-CAC contents. (b) Compressive stress of hydrogels. (c) Compressive modulus and toughness of hydrogels. (d) Images of the compression and release processes of CDs/F-CAC-1.5 under 70% deformation. (e) Stress–strain curves of the CDs/F-CAC-1.5 hydrogel under cyclic compression with a peak strain of 50% without resting time. (f) Cyclic compressive loading–unloading curves under different strains (10, 30, and 50%). (g) Dynamic oscillatory frequency sweeps of hydrogels conducted at 25 °C.

filamentous structures were observed in the CDs/F-CAC hydrogels, which contributed to denser porous structures. The swelling behavior of the hydrogels confirms this point (Figure S6). With an increase in the CDs/F-CAC content, the swelling ratio of the hydrogels decreased, indicating an increase in crosslinking density. Therefore, it can be assumed from the SEM results that massive micropores in the hydrogel network prevent the propagation of cracks, and the homogeneous pore size enables the even distribution of stress to resist force centralization.[50,51]

Mechanical Properties and Rheological Behavior. The mechanical properties of the hydrogels were evaluated using uniaxial compression tests. As shown in Figure 6a, the hydrogels do not exhibit remarkable fractures upon compression tests at up to 70% strain according to the nominal compressive strain–stress curves; they quickly recover their original state after stress unloading during the compression test, indicating that the gels have extraordinary anti-fatigue properties (Figure 6d). The results demonstrate that incorporating CDs/F-CAC significantly improves the compressibility of the P(AAm-*co*-HEMA) hydrogels, and with an increase in the CDs/F-CAC concentration, the compressive performance of the hydrogels gradually improves. Specifically, as shown in Figure 6b–c, the compressive performance of the CDs/F-CAC-0 hydrogels is the worst at 70% compressive strain, with stress, compressive modulus, and compressive toughness values of 389.87 kPa, 193.33 kPa, and 79.85 kJ/m^3, respectively. The CDs/F-CAC-1.5 hydrogels exhibited the highest strength and toughness; the stress, compressive modulus, and compressive toughness increased to 1607.30 kPa, 368.33 kPa, and 191.54 kJ/m^3, respectively. Cyclic compressive loading–unloading tests at 50% strain without any interruption were used to further investigate the fatigue resistance, resilience, and self-recovery capabilities of the CDs/F-CAC-1.5 hydrogels. From Figure 6e, the hydrogel can completely recover from 10 consecutive compression cycles and exhibit overlapping hysteresis loops, thus proving that nanocomposite hydrogels have excellent self-recovery and anti-fatigue properties.[52] At the same time, the hysteresis energy decreased slightly during the 10 consecutive compression tests but returned to its original value after the 10th compression (Figure S8). This stabilized hysteresis energy upon cyclic

https://doi.org/10.1021/acssuschemeng.3c01838
ACS Sustainable Chem. Eng. XXXX, XXX, XXX–XXX

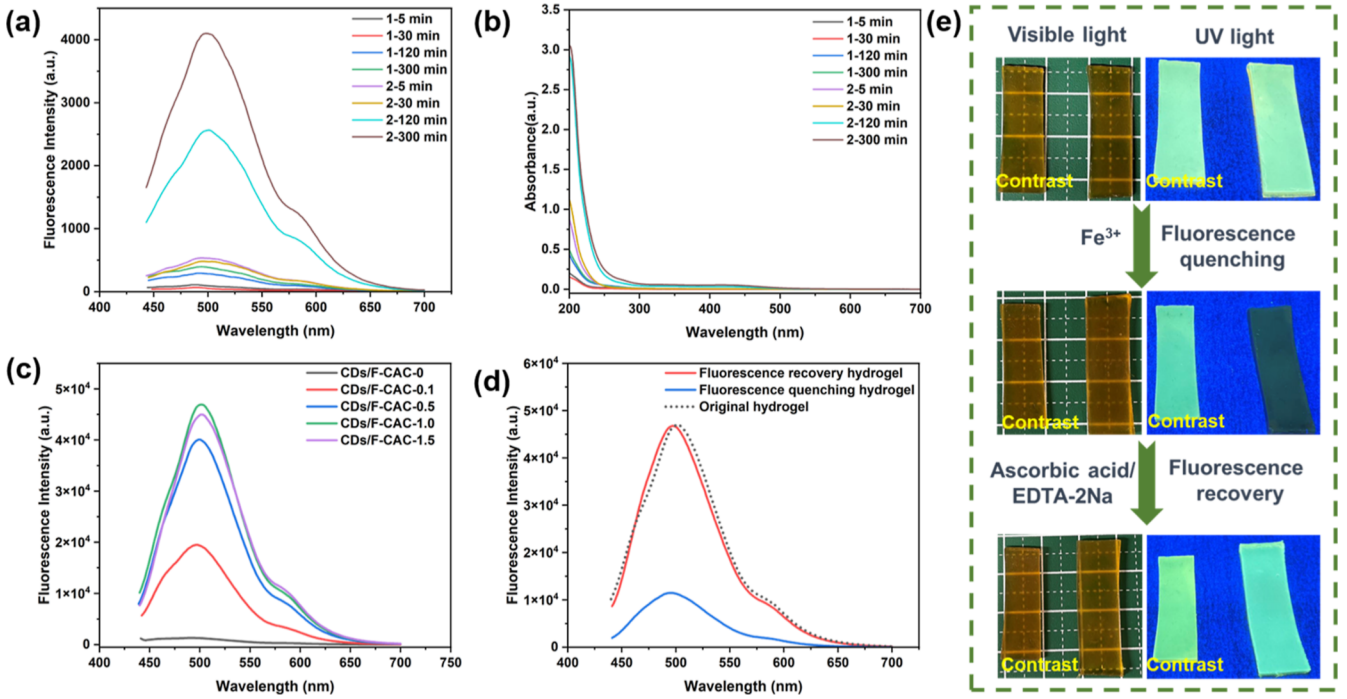

Figure 7. Characterizations of the hydrogel soaking solutions (1 represents CDs/F-CAC-1.0 hydrogel, and 2 represents CDs-1.0 hydrogel). (a) Fluorescence spectra excited at 420 nm. (b) UV−vis spectra. Fluorescent properties of hydrogels. (c) Fluorescence spectra of hydrogels with different concentrations of CDs/F-CAC excited at 420 nm. (d) Fluorescence spectra of fluorescence-quenched CDs/F-CAC-1.0 after soaking in a 125 mM $FeCl_3$ solution for 2 h and the fluorescence-recovery CDs/F-CAC-1.0 after soaking in a 0.1 M ascorbic acid/EDTA-2Na mixture (molar ratio 1:1) for 2 h, excited at 420 nm. (e) Images of fluorescence-quenched CDs/F-CAC-1.0 after soaking in a 125 mM $FeCl_3$ solution for 2 h and the fluorescence-recovery CDs/F-CAC-1.0 hydrogel after soaking in a 0.1 M ascorbic acid/EDTA-2Na mixture for 2 h under visible and UV light.

loading confirms the excellent fatigue resistance of the gels.[53] Furthermore, consecutive loading−unloading tests with gradually increasing compressive strains from 10% to 30% and 50% were performed on the same hydrogel. As shown in Figure 6f, with the increased strain, the hysteresis loop and hysteresis energy increases sharply, which is due to the rupture of noncovalent interactions between CDs/F-CAC and the polymer matrix to dissipate more energy.[50,54] The excellent mechanical properties of CDs/F-CAC hydrogels can cope with various high degrees of deformation and continuous deformation with good fatigue resistance, which is beneficial for gels utilized as flexible materials to withstand repeatable deformation.[50] To illustrate the effect of CDs/F-CAC nanomaterials on the dynamic mechanical properties of P(AAm-*co*-HEMA) hydrogels, the viscoelastic properties of these hydrogels were investigated *via* the oscillatory rheological test. Figure 6g shows the tendencies of the storage (G') and loss (G'') moduli at various frequencies under a constant low strain (0.1%). All hydrogels exhibit elastic-solid-like behavior over the entire frequency sweeping range because G' is invariably larger than G''.[31] Moreover, both G' and G'' increase with increasing CDs/F-CAC content and slightly increase with increasing oscillation frequency. The results indicate that the addition of CDs/F-CAC effectively improves the mechanical strength of hydrogels, further supporting the mechanical test results.[55,56]

Fluorescence Properties of CDs/F-CAC Hydrogels. To verify the immobilization effect of F-CAC on the CDs in the hydrogel matrix, a soaking experiment was designed and performed; it compared the CDs/F-CAC-1.0 hydrogels with CDs-1.0 hydrogels containing the same CDs mass, which was calculated based on the previous loading rate. The CDs/F-CAC-1.0 and CDs-1.0 hydrogels with the same thickness, shape, and quality were immersed in DI water of the same quality. Subsequently, the same quality of the hydrogel leaching solution was tested using UV−vis and fluorescence spectroscopy within a certain interval. As shown in Figure 7a,b, CDs-1.0 hydrogels without F-CAC are more likely to lose CDs, and the fluorescence intensity reflecting the concentration of 2 h soaking solution increases with an increase in soaking time. Even after the hydrogel reaches the swelling equilibrium state after 20 h (Figure S6), CDs are still leaching from CDs-1.0 hydrogels (Figure S9b,c). However, the fluorescence intensity of the hydrogel swollen solution (10 d) involved in chemical immobilization reaction was not significantly enhanced, which further confirmed that the addition of F-CAC can not only improve the mechanical properties of hydrogels but also immobilize and stabilize CDs in the matrix of hydrogels effectively.

The fluorescence properties of CDs/F-CAC hydrogels were further investigated and are shown in Figure 7c. Pure P(AAm-*co*-HEMA) hydrogels, which were CDs/F-CAC-0 hydrogels, exhibit no fluorescence, and the fluorescence intensity gradually increased as the CDs/F-CAC content changes from 0.1 to 1.0 wt %. However, compared with CDs/F-CAC-1.0, the fluorescence intensity of the CDs/F-CAC-1.5 hydrogel did not increase and slightly decreases. This may be attributed to the inhomogeneous dispersion of the CDs/F-CAC in the hydrogel matrix resulting from its excessive content, leading to fluorescence quenching. To verify this speculation, the fluorescence phenomenon of CDs/F-CAC dispersion solution with 0, 0.1, 0.5, 1, and 1.5 wt % was tested (Figure S10). The fluorescence intensity in solution declined from 1.0 wt %, yet the hydrogel exhibited similar fluorescence

https://doi.org/10.1021/acssuschemeng.3c01838
ACS Sustainable Chem. Eng. XXXX, XXX, XXX−XXX

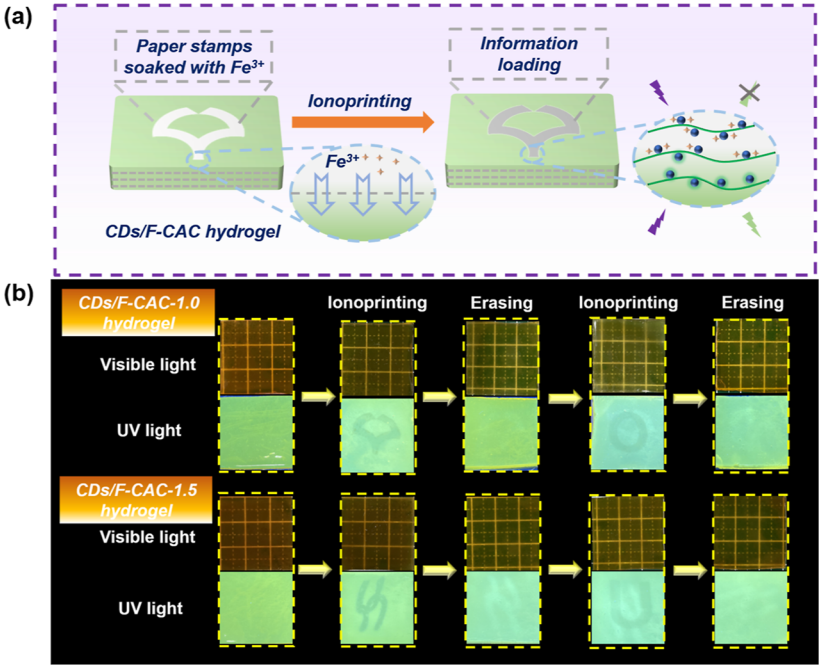

Figure 8. (a) Schematic illustration of the ionoprinting process. (b) Photos of a repeatable cycle between the ionoprinting and erasing processes of CDs/F-CAC-1.0 and CDs/F-CAC-1.5 hydrogels under visible and UV light.

variation from 1.5 wt %. In view of the similar trends, the concentration of CDs had a significant impact on fluorescence intensity, consistent with the ACQ effect.[26,57] The differences between hydrogels and solutions lie in that the ACQ effect can be suppressed *via* CDs dispersion into polymer crosslinked network (solid matrix).[58] According to a previous report,[59] the molecular fluorophore of green fluorescing CDs based on citric acid and urea was 4-hydroxy-1*H*-pyrrolo[3,4-*c*]pyridine-1,3,6-(2*H*,5*H*)-trione. Therefore, Fe^{3+} ion could interact with the aromatic hydroxyl groups and further coordinate with the amino groups,[60] causing the nonradiative electron−hole annihilation. The PL quenching can be ascribed to the transfer of electrons from the excited state to the half-filled 3d orbitals in Fe^{3+}.[61,62] Therefore, CDs-based materials can be applied to information storage, fluorescent probes, and intelligent sensing.[63] We examined the fluorescence quenching effect of Fe^{3+} on the as-prepared CDs/F-CAC luminescent hydrogels and the fluorescence recovery effect of the ascorbic acid/EDTA-2Na mixture (molar ratio 1:1) on the fluorescence-quenched hydrogels. Considering the swelling of hydrogel, the CDs/F-CAC-1.0 hydrogel was soaked in a 125 mM $FeCl_3$ solution for 2 h, and the fluorescence intensity was lower than the original hydrogel as shown in Figure 7d. Accordingly, when the hydrogel quenched with Fe^{3+} was immersed in a 0.1 M ascorbic acid/EDTA-2Na mixed solution for 2 h, the fluorescence intensity restored to near its original value (dots line, Figure 7d). This is because ascorbic acid and EDTA-2Na have better binding capabilities with Fe^{3+}, separating it from the hydrogel system.[64] In Figure 7e, these processes and changes are recorded by optical images of the CDs/F-CAC-1.0 hydrogel strips under visible and ultraviolet light and compared with the original strips.

Fluorescence-Quenching-Based Repeatable Information Loading and Anti-counterfeiting. It was verified that the fluorescence of the CDs/F-CAC hydrogels could be quenched by Fe^{3+}, and this fluorescence quenching could be eliminated using ascorbic acid/EDTA-2Na, as discussed previously. This encouraged us to explore fluorescence-quenching-based information loading and anti-counterfeiting. As shown in Figure 8a, filter papers with special shapes containing Fe^{3+} are placed on the surface of the CDs/F-CAC hydrogels for 2 min. In the process of ionoprinting, Fe^{3+} ions spontaneously diffused from the filter papers to the hydrophilic hydrogels, the fluorescence of the contact surface was quenched, and desirable patterns were remained on the surface of the CDs/F-CAC hydrogels.[35] Based on this principle, complex pattern combined with animal symbol and text was attempted to be written into the gel. In Figure S11, a panda contour and "check!" could be clearly observed after a 2 min ionoprinting process. Moreover amazingly, the patterns still retained after 7 days, even though the hydrogel had dried out due to massive water loss. This phenomenon confirmed that the graphics on the gels have an outstanding stability because of the regular diffusion of Fe^{3+}. It is of vital importance to demonstrate the spatial resolution of ionoprinted patterns, so that an array of square motifs was applied to experimentally explore the limit of feature sizes (Figure S12). Although the unevenness of the filter paper caused the large pattern to be grainy, it is visible that the fluorescent printing produced squares with desired dimensions (~500 μm) for practical applications. Specially, information loading and erasing experiments were conducted applying the CDs/F-CAC-1.0 and CDs/F-CAC-1.5 hydrogels with near-fluorescence intensity in Figure 8b. Particular patterns could be easily transferred to the surface of fluorescent hydrogels, and these printed patterns could only be observed under UV light, which can achieve the purpose of information loading and prevent information leakage.[65] Notably, the abovementioned loading information could be wiped by simply immersing the quenched hydrogels in an ascorbic acid/EDTA-2Na mixed solution, during which ascorbic acid and EDTA-2Na would bind to Fe^{3+} ions, restoring the quenched fluorescence. Correspondingly, the new

https://doi.org/10.1021/acssuschemeng.3c01838
ACS Sustainable Chem. Eng. XXXX, XXX, XXX−XXX

patterns could be imprinted and erased circularly onto the hydrogel after treatment with both $FeCl_3$ and ascorbic acid/EDTA-2Na solution. It is worth noting that the pattern is gradually difficult to be erased due to the chemical product accumulation, leading to a pattern residue caused by decreasing color-changing capacity. As far as the hydrogel swelling behavior (4 h soaking per cycle) and pattern clarity are concerned, it is reasonable for this "printing−erasing" cycle to be repeated for 5 times (Figure S13). This repeatable process indicates that CDs/F-CAC hydrogels have great potential in the field of information storage and counterfeiting. Moreover, compared with the CDs/F-CAC-1.0 hydrogels, the information loaded on the CDs/F-CAC-1.5 hydrogels were not easily erased without leaving traces. This may be due to the addition of excess CDs/F-CAC, which is consistent with the fluorescence properties.

To further evaluate the mechanical and information loading performance of the as-prepared fluorescent hydrogel, previously reported gels and films with CDs or organic dyes were selected to be compared.[13,14,23,31,63,64,66−69] As shown in Figure S14, three aspects including (i) mechanical properties: compressive stress; (ii) duplication: erasing cycles and erasability; and (iii) displaying performance: pattern resolution were demonstrated. The CDs/F-CAC hydrogel exhibited multifunctionality and superior anti-counterfeiting performance to that of most reported fluorescence flexible materials.

CONCLUSION

In summary, a novel photoluminescent cellulose-based CDs/F-CAC nanomaterial functionalized with non-toxic CDs was prepared *via* an acylation reaction. Successful preparation was confirmed by Fourier-transform infrared spectroscopy, UV−vis absorption spectroscopy, XPS, and thermal analysis. The biomass originated CDs/F-CAC hydrogels with excellent fluorescence performance were further fabricated *via* a one-pot in situ free-radical polymerization. On the one hand, the addition of CDs/F-CAC enhanced the mechanical properties of the hydrogels. With the increase in the CDs/F-CAC content from 0 to 1.5 wt %, at 70% compressive strain, the stress, compressive modulus, and compressive toughness increased from 389.87 kPa, 193.33 kPa, and 79.85 kJ/m^3 to 1607.30 kPa, 368.33 kPa, and 191.54 kJ/m^3, respectively. The CDs/F-CAC-1.5 hydrogels exhibited excellent recovery performance after the compressive loading−unloading cycling test. On the other hand, CDs/F-CAC-endowed hydrogels with exceptional fluorescent performance exhibited green fluorescence under UV light (365 nm) irradiation, and the fluorescence could be quenched or recovered *via* treatment with Fe^{3+} ions or ascorbic acid/EDTA-2Na, respectively. Thus, the CDs/F-CAC hydrogels enabled repeatable information loading and erasing through the ionoprinting method based on the fluorescence properties. The stored information could only be observed under UV light; therefore, an anti-counterfeiting effect was achieved. The excellent properties of this fluorescent hydrogel make it a promising candidate for sustainable information storage devices.

ASSOCIATED CONTENT

Supporting Information

The Supporting Information is available free of charge at https://pubs.acs.org/doi/10.1021/acssuschemeng.3c01838.

Photograph of CDs dispersion; AFM images and topography of F-CAC; fluorescence excitation and emission spectra of CDs; photostability of F-CAC, CDs and CDs/F-CAC; transmittance profiles of the hydrogel samples; swelling behavior of hydrogels; cross-sectional SEM images of the freeze-dried hydrogels; hysteresis energy of CDs/F-CAC-1.5 hydrogel; photographs, UV−vis spectra and fluorescence spectra of hydrogels in DI water immersion. Fluorescence spectra of the solutions with different concentrations of CDs/F-CAC excited at 420 nm; complex pattern and an array of square motifs on the hydrogels; fluorescence intensity change of the hydrogels at 420 nm after being treated sequentially by 125 mM $FeCl_3$ solution and 0.1 M ascorbic acid/EDTA-2Na mixed solution (5 cycles); a comparison between this work and previously reported gels and films and the table of surface chemical composition of F-CAC, CDs and CDs/F-CAC (PDF)

AUTHOR INFORMATION

Corresponding Authors

Yu-I Hsu − *Department of Applied Chemistry, Osaka University, Suita, Osaka 565-0871, Japan;* orcid.org/0000-0002-4533-7200; Email: yuihsu@chem.eng.osaka-u.ac.jp

Hiroshi Uyama − *Department of Applied Chemistry, Osaka University, Suita, Osaka 565-0871, Japan;* orcid.org/0000-0002-8587-2507; Email: uyama@chem.eng.osaka-u.ac.jp

Authors

Juan Wang − *Department of Applied Chemistry, Osaka University, Suita, Osaka 565-0871, Japan*

Peng Du − *Department of Applied Chemistry, Osaka University, Suita, Osaka 565-0871, Japan;* orcid.org/0009-0005-8661-2044

Complete contact information is available at: https://pubs.acs.org/10.1021/acssuschemeng.3c01838

Author Contributions

J.W.: Investigation, writing—original draft, writing—review and editing; P.D.: Formal analysis, writing—review and editing; Y.-I.H.: Supervision, writing—review and editing, funding acquisition; H.U.: Supervision, writing—review and editing, funding acquisition.

Notes

The authors declare no competing financial interest.

ACKNOWLEDGMENTS

This work was supported by the Japan Society for the Promotion of Science (JSPS) KAKENHI grants (no. 20H02797), New Energy and Industrial Technology Development Organization (NEDO) (JPNP 20004), and Japan Science and Technology Agency (JST) (grant number JPMJPF2218). J.W. and P.D. acknowledge support from the China Scholarship Council (CSC), China, and the Ministry of Education, Culture, Sports, Science and Technology (MEXT), Japan, for a scholarship grant.

REFERENCES

(1) Lou, K.; Hu, Z.; Zhang, H.; Li, Q.; Ji, X. Information Storage Based on Stimuli-Responsive Fluorescent 3D Code Materials. *Adv. Funct. Mater.* **2022**, *32*, 2113274.

(2) Li, M.; Lu, H.; Wang, X.; Wang, Z.; Pi, M.; Cui, W.; Ran, R. Regulable Mixed-Solvent-Induced Phase Separation in Hydrogels for Information Encryption. *Small* **2022**, *18*, 2205359.

(3) Le, X.; Shang, H.; Yan, H.; Zhang, J.; Lu, W.; Liu, M.; Wang, L.; Lu, G.; Xue, Q.; Chen, T. A Urease-Containing Fluorescent Hydrogel for Transient Information Storage. *Angew. Chem., Int. Ed.* **2021**, *60*, 3640−3646.

(4) Wang, Q.; Qi, Z.; Wang, Q.-M.; Chen, M.; Lin, B.; Qu, D.-H. A Time-Dependent Fluorescent Hydrogel for "Time-Lock" Information Encryption. *Adv. Funct. Mater.* **2022**, *32*, 2208865.

(5) Wu, H.; Chen, Y.; Liu, Y. Reversibly Photoswitchable Supramolecular Assembly and Its Application as a Photoerasable Fluorescent Ink. *Adv. Mater.* **2017**, *29*, 1605271.

(6) Kumar, P.; Singh, S.; Gupta, B. K. Future Prospects of Luminescent Nanomaterial Based Security Inks: From Synthesis to Anti-Counterfeiting Applications. *Nanoscale* **2016**, *8*, 14297−14340.

(7) Le, X.; Shang, H.; Wu, S.; Zhang, J.; Liu, M.; Zheng, Y.; Chen, T. Heterogeneous Fluorescent Organohydrogel Enables Dynamic Anti-Counterfeiting. *Adv. Funct. Mater.* **2021**, *31*, 2108365.

(8) Khlifi, S.; Fournier Le Ray, N.; Paofai, S.; Amela-Cortes, M.; Akdas-Kiliç, H.; Taupier, G.; Derien, S.; Cordier, S.; Achard, M.; Molard, Y. Self-Erasable Inkless Imprinting Using a Dual Emitting Hybrid Organic-Inorganic Material. *Mater. Today* **2020**, *35*, 34−41.

(9) Liu, Y.; Zhao, K.; Ren, Y.; Wan, S.; Yang, C.; Li, J.; Wang, F.; Chen, C.; Su, J.; Chen, D.; Zhao, Y.; Liu, K.; Zhang, H. Highly Plasticized Lanthanide Luminescence for Information Storage and Encryption Applications. *Adv. Sci.* **2022**, *9*, 2105108.

(10) Pan, G.; Yan, J.; Tang, Z.; Zhang, J.; Lin, X.; Yang, D.; Wu, J.; Lin, W.; Yi, G. A Hybrid Hydrogel System Composed of CdTe Quantum Dots and Photonic Crystals for Optical Anti-Counterfeiting and Information Encoding−Decoding. *J. Mater. Chem. C* **2022**, *10*, 3959−3970.

(11) Zhao, W.; Li, H.; Chen, Y.; Yang, D. Cu^{2+}-Induced "Off−on−Off" Switching Luminescence of Cellulose-Based Luminescent Hydrogels. *ACS Sustainable Chem. Eng.* **2023**, *11*, 4509−4516.

(12) Su, G.; Li, Z.; Gong, J.; Zhang, R.; Dai, R.; Deng, Y.; Tang, B. Z. Information-Storage Expansion Enabled by a Resilient Aggregation-Induced-Emission-Active Nanocomposite Hydrogel. *Adv. Mater.* **2022**, *34*, 2207212.

(13) Wang, J.; Zhang, M.; Han, S.; Zhu, L.; Jia, X. Multiple-Stimuli-Responsive Multicolor Luminescent Self-Healing Hydrogel and Application in Information Encryption and Bioinspired Camouflage. *J. Mater. Chem. C* **2022**, *10*, 15565−15572.

(14) Li, P.; Zhang, D.; Zhang, Y.; Lu, W.; Zhang, J.; Wang, W.; He, Q.; Théato, P.; Chen, T. Aggregation-Caused Quenching-Type Naphthalimide Fluorophores Grafted and Ionized in a 3D Polymeric Hydrogel Network for Highly Fluorescent and Locally Tunable Emission. *ACS Macro Lett.* **2019**, *8*, 937−942.

(15) Chen, Z.; Chen, Y.; Guo, Y.; Yang, Z.; Li, H.; Liu, H. Paper-Structure Inspired Multiresponsive Hydrogels with Solvent-Induced Reversible Information Recording, Self-Encryption, and Multi-decryption. *Adv. Funct. Mater.* **2022**, *32*, 2201009.

(16) Lou, D.; Sun, Y.; Li, J.; Zheng, Y.; Zhou, Z.; Yang, J.; Pan, C.; Zheng, Z.; Chen, X.; Liu, W. Double Lock Label Based on Thermosensitive Polymer Hydrogels for Information Camouflage and Multilevel Encryption. *Angew. Chem., Int. Ed.* **2022**, *61*, No. e202117066.

(17) Liu, J.; Chen, Z.; Chen, Y.; Rehman, H. U.; Guo, Y.; Li, H.; Liu, H. Ionic Conductive Organohydrogels with Dynamic Pattern Behavior and Multi-Environmental Stability. *Adv. Funct. Mater.* **2021**, *31*, 2101464.

(18) Bicak, T. C.; Garnier, M.; Sabbah, M.; Griffete, N. Photoinduced Synthesis of Fluorescent Hydrogels without Fluorescent Monomers. *Chem. Commun.* **2022**, *58*, 9614−9617.

(19) Wang, J.; Nan, J.; Li, M.; Yuan, G.; Zhao, Y.; Dai, J.; Zhang, K. First Evidence of Contamination in Aquatic Organisms with Organic Light-Emitting Materials. *Environ. Sci. Technol. Lett.* **2022**, *9*, 739−746.

(20) Rasal, A. S.; Yadav, S.; Yadav, A.; Kashale, A. A.; Manjunatha, S. T.; Altaee, A.; Chang, J.-Y. Carbon Quantum Dots for Energy Applications: A Review. *ACS Appl. Nano Mater.* **2021**, *4*, 6515−6541.

(21) Manikandan, V.; Lee, N. Y. Green Synthesis of Carbon Quantum Dots and Their Environmental Applications. *Environ. Res.* **2022**, *212*, 113283.

(22) Qiu, J.; Ye, W.; Xu, X.; Chen, C.; Xu, Z.; Lei, B.; Hu, C.; Zhuang, J.; Dong, H.; Guangqi, H.; Liu, Y. One-Step Hydrothermal Synthesis of Nitrogen-Doped Carbonized Polymer Dots with Full-Band Absorption for Skin Protection. *ACS Sustainable Chem. Eng.* **2022**, *10*, 11958−11968.

(23) Xiong, R.; Yu, S.; Smith, M. J.; Zhou, J.; Krecker, M.; Zhang, L.; Nepal, D.; Bunning, T. J.; Tsukruk, V. V. Self-Assembly of Emissive Nanocellulose/Quantum Dot Nanostructures for Chiral Fluorescent Materials. *ACS Nano* **2019**, *13*, 9074−9081.

(24) Wu, Y.; Ren, Y.; Guo, J.; Liu, Z.; Liu, L.; Yan, F. Imidazolium-Type Ionic Liquid-Based Carbon Quantum Dot Doped Gels for Information Encryption. *Nanoscale* **2020**, *12*, 20965−20972.

(25) Sui, B.; Li, Y.; Yang, B. Nanocomposite Hydrogels Based on Carbon Dots and Polymers. *Chin. Chem. Lett.* **2020**, *31*, 1443−1447.

(26) Wang, Y.; Lv, T.; Yin, K.; Feng, N.; Sun, X.; Zhou, J.; Li, H. Carbon Dot-Based Hydrogels: Preparations, Properties, and Applications. *Small* **2023**, *19*, 2207048.

(27) Zhang, J.; Jin, J.; Wan, J.; Jiang, S.; Wu, Y.; Wang, W.; Gong, X.; Wang, H. Quantum Dots-Based Hydrogels for Sensing Applications. *Chem. Eng. J.* **2021**, *408*, 127351.

(28) Guo, X.; Xu, D.; Yuan, H.; Luo, Q.; Tang, S.; Liu, L.; Wu, Y. A Novel Fluorescent Nanocellulosic Hydrogel Based on Carbon Dots for Efficient Adsorption and Sensitive Sensing in Heavy Metals. *J. Mater. Chem. A* **2019**, *7*, 27081−27088.

(29) Liu, J.; Wang, H.; Liu, T.; Wu, Q.; Ding, Y.; Ou, R.; Guo, C.; Liu, Z.; Wang, Q. Multimodal Hydrogel-Based Respiratory Monitoring System for Diagnosing Obstructive Sleep Apnea Syndrome. *Adv. Funct. Mater.* **2022**, *32*, 2204686.

(30) Yao, X.; Zhang, S.; Qian, L.; Wei, N.; Nica, V.; Coseri, S.; Han, F. Super Stretchable, Self-Healing, Adhesive Ionic Conductive Hydrogels Based on Tailor-Made Ionic Liquid for High-Performance Strain Sensors. *Adv. Funct. Mater.* **2022**, *32*, 2204565.

(31) Lv, H.; Wang, S.; Wang, Z.; Meng, W.; Han, X.; Pu, J. Fluorescent Cellulose-Based Hydrogel with Carboxymethyl Cellulose and Carbon Quantum Dots for Information Storage and Fluorescent Anti-Counterfeiting. *Cellulose* **2022**, *29*, 6193−6204.

(32) Zhang, K.; Shi, Y.; Jia, Y.; Li, P.; Zhang, X.; Feng, X.; Zhu, L.; Sun, Y.; Hu, W.; Zhao, G. Tunable Dual Fluorescence Emissions with High Photoluminescence Quantum Yields Modulated by Na Ion Dispersion Method for Purely Solid State N-Doped Carbon Dots. *J. Photochem. Photobiol., A* **2020**, *397*, 112548.

(33) Cui, X.; Honda, T.; Asoh, T.-A.; Uyama, H. Cellulose Modified by Citric Acid Reinforced Polypropylene Resin as Fillers. *Carbohydr. Polym.* **2020**, *230*, 115662.

(34) Soni, R.; Asoh, T.-A.; Hsu, Y.-I.; Uyama, H. Freshwater-Durable and Marine-Degradable Cellulose Nanofiber Reinforced Starch Film. *Cellulose* **2022**, *29*, 1667−1678.

(35) Le, X.-X.; Lu, W.; He, J.; Serpe, M. J.; Zhang, J.-W.; Chen, T. Ionoprinting Controlled Information Storage of Fluorescent Hydrogel for Hierarchical and Multi-Dimensional Decryption. *Sci. China Mater.* **2019**, *62*, 831−839.

(36) Zhang, X.; Lu, J.; Zhou, X.; Guo, C.; Wang, C. Rapid Microwave Synthesis of N-Doped Carbon Nanodots with High Fluorescence Brightness for Cell Imaging and Sensitive Detection of Iron (III). *Opt. Mater.* **2017**, *64*, 1−8.

(37) Kondo, T.; Kose, R.; Naito, H.; Kasai, W. Aqueous Counter Collision Using Paired Water Jets as a Novel Means of Preparing Bio-Nanofibers. *Carbohydr. Polym.* **2014**, *112*, 284−290.

https://doi.org/10.1021/acssuschemeng.3c01838
ACS Sustainable Chem. Eng. XXXX, XXX, XXX−XXX

(38) Zhao, P.; Jin, B.; Zhang, Q.; Peng, R. High-Quality Carbon Nitride Quantum Dots on Photoluminescence: Effect of Carbon Sources. *Langmuir* **2021**, *37*, 1760−1767.
(39) Meierhofer, F.; Dissinger, F.; Weigert, F.; Jungclaus, J.; Müller-Caspary, K.; Waldvogel, S. R.; Resch-Genger, U.; Voss, T. Citric Acid Based Carbon Dots with Amine Type Stabilizers: pH-Specific Luminescence and Quantum Yield Characteristics. *J. Phys. Chem. C* **2020**, *124*, 8894−8904.
(40) Cui, K.; Chang, Y.; Liu, P.; Yang, L.; Liu, T.; Zheng, Z.; Guo, Y.; Ma, X. Cell-Tailored Silicon Nanoparticles with Ultrahigh Fluorescence and Photostability for Cellular Imaging. *ACS Sustainable Chem. Eng.* **2020**, *8*, 17439−17446.
(41) Shejale, K. P.; Jaiswal, A.; Kumar, A.; Saxena, S.; Shukla, S. Nitrogen Doped Carbon Quantum Dots as Co-Active Materials for Highly Efficient Dye Sensitized Solar Cells. *Carbon* **2021**, *183*, 169−175.
(42) Wang, L.; Zhang, X.; Yang, K.; Wang, L.; Lee, C.-S. Oxygen/Nitrogen-Related Surface States Controlled Carbon Nanodots with Tunable Full-Color Luminescence: Mechanism and Bio-Imaging. *Carbon* **2020**, *160*, 298−306.
(43) Shen, J.; Zhu, Y.; Yang, X.; Zong, J.; Zhang, J.; Li, C. One-Pot Hydrothermal Synthesis of Graphene Quantum Dots Surface-Passivated by Polyethylene Glycol and Their Photoelectric Conversion under near-Infrared Light. *New J. Chem.* **2012**, *36*, 97−101.
(44) Zou, W.; Ma, X.; Zheng, P. Preparation and Functional Study of Cellulose/Carbon Quantum Dot Composites. *Cellulose* **2020**, *27*, 2099−2113.
(45) Xue, B.; Yang, Y.; Tang, R.; Sun, Y.; Sun, S.; Cao, X.; Li, P.; Zhang, Z.; Li, X. One-Step Hydrothermal Synthesis of a Flexible Nanopaper-Based Fe^{3+} Sensor Using Carbon Quantum Dot Grafted Cellulose Nanofibrils. *Cellulose* **2020**, *27*, 729−742.
(46) Li, X.; Hu, Y. Luminescent Films Functionalized with Cellulose Nanofibrils/CdTe Quantum Dots for Anti-Counterfeiting Applications. *Carbohydr. Polym.* **2019**, *203*, 167−175.
(47) Guo, J.; Liu, D.; Filpponen, I.; Johansson, L.-S.; Malho, J.-M.; Quraishi, S.; Liebner, F.; Santos, H. A.; Rojas, O. J. Photoluminescent Hybrids of Cellulose Nanocrystals and Carbon Quantum Dots as Cytocompatible Probes for in Vitro Bioimaging. *Biomacromolecules* **2017**, *18*, 2045−2055.
(48) Huang, J.; Liu, X.; Li, L.; Chen, S.; Yang, J.; Yan, J.; Xu, F.; Zhang, X. Nitrogen-Doped Carbon Quantum Dot-Anchored Hydrogels for Visual Recognition of Dual Metal Ions through Reversible Fluorescence Response. *ACS Sustainable Chem. Eng.* **2021**, *9*, 15190−15201.
(49) Chen, X.; Song, Z.; Yuan, B.; Li, X.; Li, S.; Thang Nguyen, T.; Guo, M.; Guo, Z. Fluorescent Carbon Dots Crosslinked Cellulose Nanofibril/Chitosan Interpenetrating Hydrogel System for Sensitive Detection and Efficient Adsorption of Cu (II) and Cr (VI). *Chem. Eng. J.* **2022**, *430*, 133154.
(50) Shao, C.; Wang, M.; Chang, H.; Xu, F.; Yang, J. A Self-Healing Cellulose Nanocrystal-Poly(ethylene glycol) Nanocomposite Hydrogel via Diels−Alder Click Reaction. *ACS Sustainable Chem. Eng.* **2017**, *5*, 6167−6174.
(51) Hao, S.; Shao, C.; Meng, L.; Cui, C.; Xu, F.; Yang, J. Tannic Acid−Silver Dual Catalysis Induced Rapid Polymerization of Conductive Hydrogel Sensors with Excellent Stretchability, Self-Adhesion, and Strain-Sensitivity Properties. *ACS Appl. Mater. Interfaces* **2020**, *12*, 56509−56521.
(52) Wu, M.; Pan, M.; Qiao, C.; Ma, Y.; Yan, B.; Yang, W.; Peng, Q.; Han, L.; Zeng, H. Ultra Stretchable, Tough, Elastic and Transparent Hydrogel Skins Integrated with Intelligent Sensing Functions Enabled by Machine Learning Algorithms. *Chem. Eng. J.* **2022**, *450*, 138212.
(53) Du, G.; Gao, G.; Hou, R.; Cheng, Y.; Chen, T.; Fu, J.; Fei, B. Tough and Fatigue Resistant Biomimetic Hydrogels of Interlaced Self-Assembled Conjugated Polymer Belts with a Polyelectrolyte Network. *Chem. Mater.* **2014**, *26*, 3522−3529.
(54) Meng, L.; Shao, C.; Cui, C.; Xu, F.; Lei, J.; Yang, J. Autonomous Self-Healing Silk Fibroin Injectable Hydrogels Formed via Surfactant-Free Hydrophobic Association. *ACS Appl. Mater. Interfaces* **2020**, *12*, 1628−1639.
(55) Nian, G.; Kim, J.; Bao, X.; Suo, Z. Making Highly Elastic and Tough Hydrogels from Doughs. *Adv. Mater.* **2022**, *34*, 2206577.
(56) Du, P.; Wang, J.; Hsu, Y.-I.; Uyama, H. Bio-Inspired Homogeneous Conductive Hydrogel with Flexibility and Adhesiveness for Information Transmission and Sign Language Recognition. *ACS Appl. Mater. Interfaces* **2023**, *15*, 23711−23724.
(57) Chen, B.; Wang, F. Combating Concentration Quenching in Upconversion Nanoparticles. *Acc. Chem. Res.* **2020**, *53*, 358−367.
(58) Qu, Y.-F.; Li, D.; Qu, S.-N. Solid-State Luminescent Carbon Dots Resistant to Aggregation-Induced Fluorescence Quenching: Preparation, Photophysical Properties and Applications. *Chin. J. Lumin.* **2021**, *42*, 1141−1154.
(59) Kasprzyk, W.; Świergosz, T.; Bednarz, S.; Walas, K.; Bashmakova, N. V.; Bogdał, D. Luminescence Phenomena of Carbon Dots Derived from Citric Acid and Urea − a Molecular Insight. *Nanoscale* **2018**, *10*, 13889−13894.
(60) Omer, K. M.; Tofiq, D. I.; Hassan, A. Q. Solvothermal Synthesis of Phosphorus and Nitrogen Doped Carbon Quantum Dots as a Fluorescent Probe for Iron(III). *Microchim. Acta* **2018**, *185*, 466.
(61) Song, Y.; Zhu, C.; Song, J.; Li, H.; Du, D.; Lin, Y. Drug-Derived Bright and Color-Tunable N-Doped Carbon Dots for Cell Imaging and Sensitive Detection of Fe^{3+} in Living Cells. *ACS Appl. Mater. Interfaces* **2017**, *9*, 7399−7405.
(62) Zhu, S.; Meng, Q.; Wang, L.; Zhang, J.; Song, Y.; Jin, H.; Zhang, K.; Sun, H.; Wang, H.; Yang, B. Highly Photoluminescent Carbon Dots for Multicolor Patterning, Sensors, and Bioimaging. *Angew. Chem., Int. Ed.* **2013**, *52*, 3953−3957.
(63) Qiu, Z.; Wang, X.; Wang, T.; Zhao, X.; Zhang, J.; Xu, C.; Xu, J.; Yin, H. Stretchable and Self-Healable Double-Network Ionogel with Strong Adhesion and Temperature Tolerance for Information Encryption. *J. Mol. Liq.* **2022**, *351*, 118626.
(64) Liu, Y.; Zhang, Z.; Liang, Z.; Yong, Y.; Yang, C.; Li, Z. Multifunctional Polyurethane Hydrogel Based on a Phenol−Carbamate Network and an Fe^{3+}−Polyphenol Coordination Bond toward NIR Light Triggered Actuators and Strain Sensors. *J. Mater. Chem. A* **2022**, *10*, 16928−16940.
(65) Wu, B.-Y.; Le, X.-X.; Jian, Y.-K.; Lu, W.; Yang, Z.-Y.; Zheng, Z.-K.; Théato, P.; Zhang, J.-W.; Zhang, A.; Chen, T. Ph and Thermo Dual-Responsive Fluorescent Hydrogel Actuator. *Macromol. Rapid Commun.* **2019**, *40*, 1800648.
(66) Li, C. Y.; Zheng, S. Y.; Du, C.; Ling, J.; Zhu, C. N.; Wang, Y. J.; Wu, Z. L.; Zheng, Q. Carbon Dot/Poly(methylacrylic acid) Nanocomposite Hydrogels with High Toughness and Strong Fluorescence. *ACS Appl. Polym. Mater.* **2020**, *2*, 1043−1052.
(67) Xie, S.; Chen, Y.; Guo, Z.; Luo, Y.; Tan, H.; Xu, L.; Xu, J.; Zheng, J. Agar/Carbon Dot Crosslinked Polyacrylamide Double-Network Hydrogels with Robustness, Self-Healing, and Stimulus-Response Fluorescence for Smart Anti-Counterfeiting. *Mater. Chem. Front.* **2021**, *5*, 5418−5428.
(68) Hou, L. X.; Ding, H.; Hao, X. P.; Zhu, C. N.; Du, M.; Wu, Z. L.; Zheng, Q. Multi-Level Encryption of Information in Morphing Hydrogels with Patterned Fluorescence. *Soft Matter* **2022**, *18*, 2149−2156.
(69) Deng, J.; Wu, H.; Xie, W.; Jia, H.; Xia, Z.; Wang, H. Metal Cation-Responsive and Excitation-Dependent Nontraditional Multicolor Fluorescent Hydrogels for Multidimensional Information Encryption. *ACS Appl. Mater. Interfaces* **2021**, *13*, 39967−39975.

https://doi.org/10.1021/acssuschemeng.3c01838
ACS Sustainable Chem. Eng. XXXX, XXX, XXX−XXX